A Simple Method to Tune Up Screen-Printed Carbon Electrodes Applicable to the Design of Disposable Electrochemical Sensors

Ya-Ling Su, *Chun-Yen Tai*, *Jyh-Myng Zen**

Department of Chemistry, National Chung Hsing University, Taichung 402, Taiwan
*e-mail: jmzen@dragon.nchu.edu.tw

Received: August 4, 2013
Accepted: September 15, 2013
Published online: October 31, 2013

Abstract
We report an easy method to tune up screen-printed carbon electrodes (SPCEs) for application in fabricating disposable electrochemical sensors. Simply by ultrasonic polishing a bare SPCE in a γ-Al_2O_3 slurry, the surface roughness was drastically smoothed coupled with a large increase in hydrophilicity. The as-generated micromorphology on the surface of the SPCE was found to be ideal for the immobilization of catechol to minimize the overpotential in the sensitive detection of nicotinamide adenine dinucleotide (NADH) and hydrazine. Physical characterization by both XPS and AFM studies specify that the adsorption behavior is related to the carbon surface functionalities and the trapping of γ-Al_2O_3 on the polished-SPCE.

Keywords: Ultrasonic polishing, γ-Al_2O_3, Catechol, NADH, Hydrazine

DOI: 10.1002/elan.201300382

1 Introduction

Immobilization of catechol and its derivatives on an "activated" carbon surface has received considerable attention for minimizing the overpotential in the electroanalysis of nicotinamide adenine dinucleotide (NADH), penicillamine, methimazole, and hydrazine [1–5]. Nonetheless, earlier studies in this research area were conducted mainly on glassy carbon electrodes (GCE) and hence the results may not be able extend to disposable electrochemical sensors. Besides, the main problem lies therein, that complicated processes are necessary to activate GCEs for catechol immobilization [6,7]. For example, in one case the electrode was first treated with a radio frequency plasma under O_2 pressure of 150 mTorr for 5 min to form the carbonyl functionality followed by reacting with 3,4-dihydroxybenzylamine in dicyclohexylcarbodiimide solvent for 60–68 h to form an amide linkage [6]. In another case, the GCE was first preanodized at 1.8 V vs. Ag/AgCl for 5 min in a pH 7 buffer. Then the catechol solution (25 mM, 1 μL) was spread over the surface, dried under hot air followed by cathodization at −1.5 V vs. Ag/AgCl for ~1 min [7]. Typical catechol immobilization can then be electrochemically prepared in catechol solution following the formation of an activated carbon surface. To simplify the activation process, we recently reported an electrochemical oxidation procedure for selective and direct immobilization of catechol on GCE and screen-printed carbon electrode (SPCE) surfaces in aqueous solutions without any other external matrix [8]. However, there is an instability problem of the activated surface, as confirmed from the potential-cycling studies, to restrict its practical applicability.

In this paper, we focus the study on disposable SPCE and advance the adsorption of catechol with a simple ultrasonic polishing and preanodization process. Physical characterization studies specify that the adsorption behavior is related to the carbon surface functionalities and trapping of γ-Al_2O_3 on the polished-SPCE. With an improved micromorphology on the polished-SPCE, further progress for the direct immobilization of catechol was achieved through preanodization of the polished-SPCE. This catechol-immobilized electrode is cheap and hence can be developed for use as disposable chemical sensors. Finally, the as-prepared electrode is demonstrated for sensitive detection of NADH and hydrazine. Since SPCE is designated for mass production [9,10], the proposed process opens a useful methodology in the field of electrochemical sensors.

2 Experimental

All chemicals were purchased at the analytical grade available and used directly without any further purification. The sources were α-Al_2O_3 (Seedchem Company Pty. Ltd., 99%), γ-Al_2O_3 (Strem Chemicals, Inc., 96%), hydrazine (Sigma-Aldrich, 99.9%), NADH (Sigma-Aldrich, HPLC grade, 97%), Na_2HPO_4 (Showa, 99%), NaH_2PO_4 (Showa, 98%), acetic acid (ECHO Chemical Co. Ltd., HPLC grade, 99.9%), and hydrochloric acid (Scharlau Chemie, 37%). All aqueous solutions were prepared with

 © 2013 Wiley-VCH Verlag GmbH & Co. KGaA, Weinheim

www.spm.com.cn

Millipore deionized water (18 MΩ cm^{-1}). A 0.1 M, pH 7 PBS was used as supporting electrolyte for electrochemical experiments. The electrode surface morphology was examined with a field-emission scanning electron microscope (SEM, JEOL JSM-6700F) with an accelerating voltage of 3 kV. The AFM images were recorded with a multimode scanning probe microscope system operated in tapping mode using Being Nano-Instruments CSPM-4000 (Ben Yuan Ltd., China). The water contact angle was measured by the static sessile drop method with a Rame–Hart Model 100 goniometer (Mt. Lakes, NJ, USA). Electrochemical experiments were conducted in a standard three-electrode cell at room temperature using a CHI 824B electrochemical analyzer (CH Instruments, USA). The three-electrode system consists of an SPCE as the working electrode (geometric area, 0.196 cm^2), an Ag/AgCl reference electrode, and a platinum auxiliary electrode.

Disposable SPCEs were obtained from Zensor R&D (Taichung, Taiwan). Abrasives of γ-Al_2O_3 at 50 % mass concentration mixed with 0.1 M, pH 2 acetate buffer solution was used as a slurry in the ultrasonic polishing process with an ultrasonic cleaner (DELTA DC200H). As to the preparation of the polished-SPCE (designated as SPCE-P), a bare SPCE was first sonicated in the slurry for 30 min. After washing with copious amounts of ultrapure water, it was sonicated again in ultrapure water for 5 min. Preanodized SPCE and SPCE-P (designated as SPCE* and SPCE-P*, respectively) were obtained by applying a potential of 2.0 V vs. Ag/AgCl for 60 s in pH 7 PBS and then cleaned by the same procedure as that of SPCE-P. Typical catechol-adsorbed SPCE-P, SPCE-P*, and SPCE*, designated as SPCE-P-CA_{ads}, SPCE-P*-CA_{ads}, and SPCE*-CA_{ads}, respectively, were prepared by continuous scanning of the respective SPCE-P, SPCE-P*, and SPCE* in 1 mM catechol at 100 mV/s (n = 25) in the potential window of −0.4–1.0 V vs. Ag/AgCl.

3 Results and Discussion

3.1 Surface Characterization of the SPCE-P

Figure 1 compares the SEM, XPS, and AFM results of a bare SPCE before/after the polishing process. As can be seen, both the SEM and AFM pictures clearly indicate that the rough surface of SPCE has been smoothed during the ultrasonic polishing process. More precisely, the surface roughness (R_a), which is the mean height as calculated over the entire measured area, was measured to improve from 22.5 nm to 7.15 nm after the ultrasonic polishing treatment. We suspect that some of the abrasive particles may become trapped at the surface layer. To address this issue, we conducted XPS analyses for a bare SPCE before/after the ultrasonic polishing process. The fact that the Al_{2s} and Al_{2p} peaks can only be observed at the SPCE-P confirms that a trace amount of the polishing material (i.e., γ-Al_2O_3) is indeed trapped on the SPCE-P surface. It is possible that the pores, holes, and defects in the surface have been blocked/partially filled by electroinactive γ-Al_2O_3 particles. As a result, surely the surface will appear more homogenous, due to the obstruction of the signals from the holes and pores on the SPCE which contain carbon in different bonding environments. Meanwhile, the ultrasonic process may also induce numerous

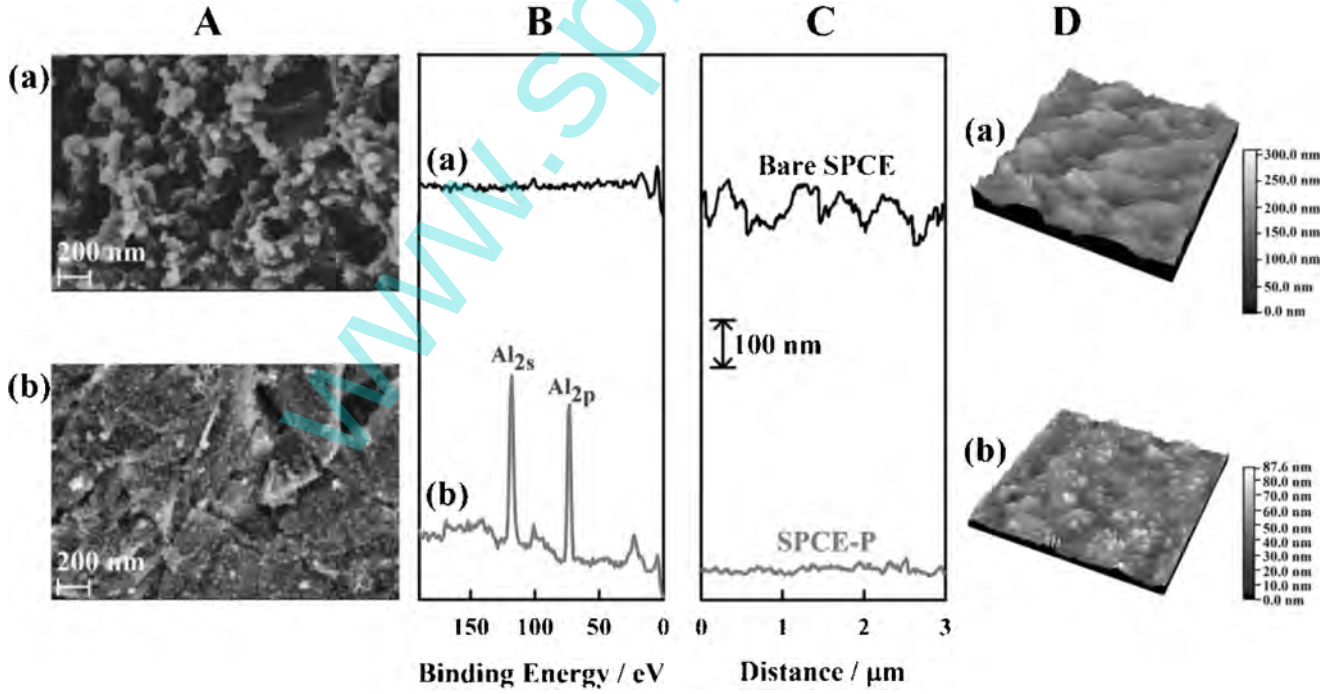

Fig. 1. The SEM images (A), XPS spectra (B), AFM surface outlines (C), and images (D) of a bare SPCE before (a) and after (b) the polishing process.

www.spm.com.cn

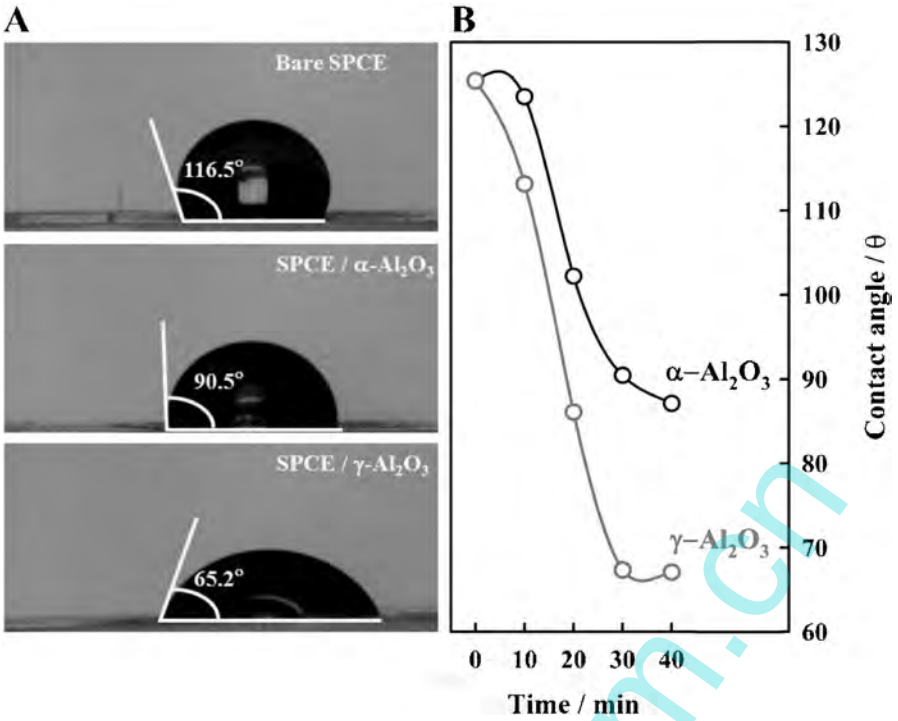

Fig. 2. Water contact angles for different SPCEs (A) and as a function of ultrasonic polishing time in γ-Al_2O_3 and α-Al_2O_3 slurries (B).

repetitive microcuts and then to further improve the micromorphology and surface roughness of the SPCE. Overall, the proposed polishing technique is capable of improving the micromorphology and surface roughness of the SPCE surface.

Earlier, a 30% α-Al_2O_3 dispersed GCE was reported to strongly adsorb compounds such as catechols and catalyze their oxidation [11,12]. With the successfully trap of γ-Al_2O_3 on the SPCE-P surface, we anticipate that by ultrasonic-polishing SPCE in α-Al_2O_3 should provide an ideal surface for catechol immobilization. We first conducted an experiment to measure the water contact angle (θ) by a goniometer since the surfaces of both SPCE-Ps were found to become more hydrophilic than that of a bare SPCE. As shown in Figure 2A, the value of θ increases in the order of: γ-Al_2O_3 polished SPCE ($\theta = 67.3^\circ$) < α-Al_2O_3 polished SPCE ($\theta = 90.5^\circ$) < a bare SPCE ($\theta = 115^\circ$). It is clear that the ultrasonic polishing treatment improves the SPCE wettability, especially in γ-Al_2O_3. Figure 2B further compares the value of θ as a function of ultrasonic polishing time in γ-Al_2O_3 and α-Al_2O_3 slurries. The measured θ values were found to decrease gradually with the increase in the polishing time up to 30 min and reached a plateau afterwards. To improve the micromorphology and surface roughness on the SPCE, it takes time for the γ-Al_2O_3 particles to fill the pores, holes, and defects in the surface with numerous repetitive microcuts during the ultrasonic process. To our surprise, the SPCE-P prepared in γ-Al_2O_3 performs much better in catechol immobilization than that of the SPCE-P prepared in a α-Al_2O_3 slurry. This is interesting since γ-Al_2O_3 is regarded as a poorer catalyst than α-Al_2O_3 and only a small amount of ~1.21% γ-Al_2O_3 was trapped on the SPCE-P [19]. Ultimately, since good hydrophilicity is required to integrate biological redox mediators, the as-prepared SPCE-P is thus very suitable for bioapplications.

3.2 Voltammetric Response of Catechol on the SPCE-P*

To prove the usefulness of the SPCE-P, a model ferri/ferrocyanide redox couple was chosen as a probe to investigate the change in electrode behavior of the SPCE-P*. As shown in Figure 3A, sluggish electron-transfer kinetics with a peak-to-peak separation (ΔE_p) value of near 290 mV was observed at a bare SPCE. Both the SPCE-P and SPCE-P* were found to show facile electron-transfer kinetics by improving the ΔE_p to 150 mV and 90 mV, respectively. Meanwhile, the highest redox peak current was also observed at the SPCE-P*. We next conducted EIS experiments to understand the chemical transformation and process associated with the SPCE-P*. Figure 3B compares the EIS results of SPCE-P*, SPCE-P, and a bare SPCE in the presence of the redox probe. As expected, the highest charge transfer resistance (R_{ct}) of ~7.89 kΩ was observed at a bare SPCE. While the R_{ct} decreased by 58.3% to 3.29 kΩ at the SPCE-P and further lowered to R_{ct} of 2.06 kΩ for the SPCE-P*. The facile electron-transfer kinetics of $K_3Fe(CN)_6$ at the SPCE-P* validates its potential for sensing applications.

After conducting the effective EIS experiments for probing the interfacial properties of electrodes, we stud-

www.sjm.com.cn

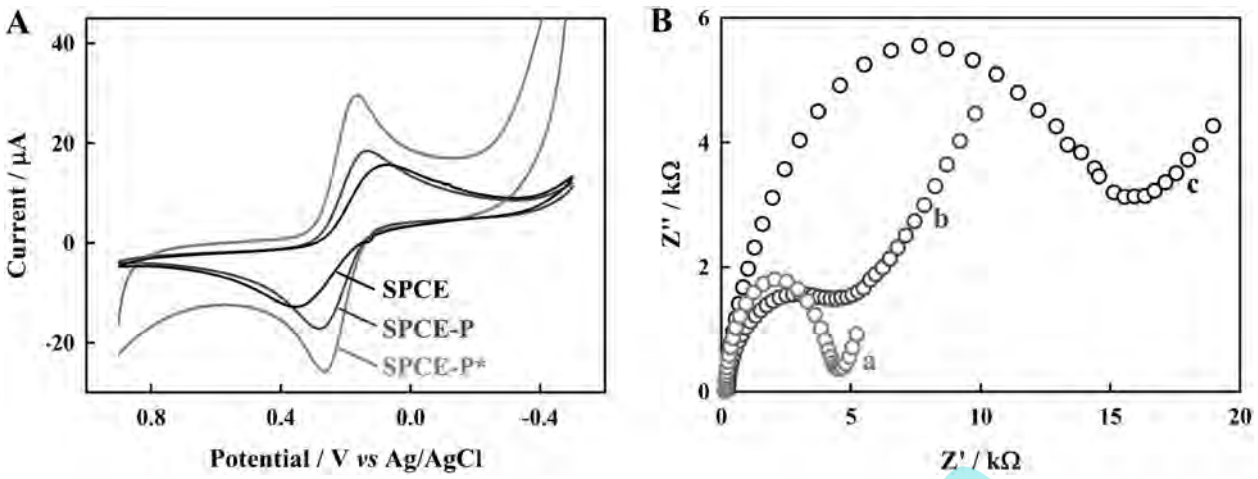

Fig. 3. (A) Cyclic voltammograms in 1 mM potassium ferrocyanide with 0.1 M KCl as supporting electrolyte at a potential scan rate of 50 $mV s^{-1}$ for different modified electrode. (B) Electrochemical impedance spectroscopy (EIS) of (a) SPCE-P*, (b) SPCE-P and (c) bare SPCE in 1 mM potassium ferrocyanide with 0.1 M KCl at a bias potential of 0.171 V.

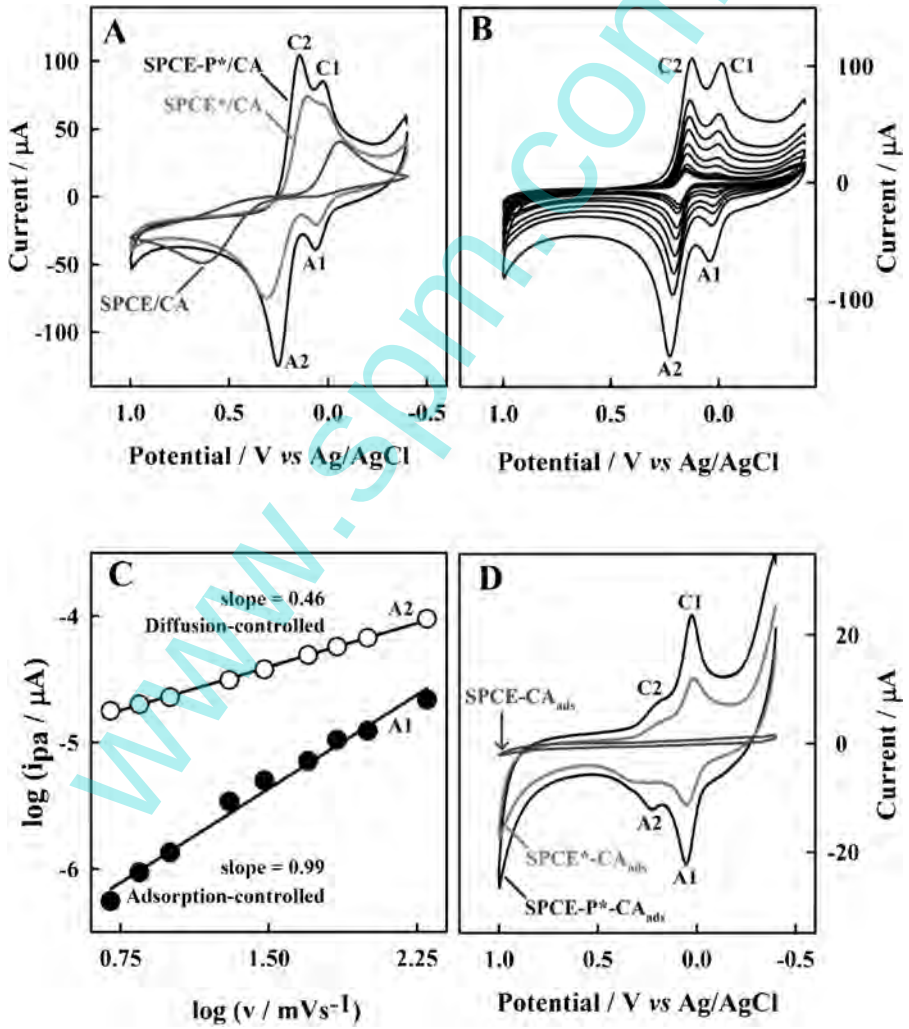

Fig. 4. (A) Cyclic voltammograms of 500 μM catechol at a bare SPCE, the SPCE*, and the SPCE-P* at a scan rate of 50 $mV s^{-1}$. (B) Cyclic voltammograms on the SPCE-P* in pH 7 PBS at different scan rates. (C) Double logarithmic plots of i_{pa} vs. scan rate. (D) Comparative CV responses of a bare SPCE, the SPCE*, and the SPCE-P* at a scan rate of 50 mV/s after medium exchange to pH 7 PBS.

www.spm.com.cn

ied the electrochemical response of 1 mM catechol at different electrodes. As shown in Figure 4A, only one redox peak ($E^{\circ\prime}=347.5$ mV, $\triangle E_p=695.0$ mV) was observed on a bare SPCE; whereas, two well-defined redox peaks of A1/C1 ($E^{\circ\prime}=43.5$ mV) and A2/C2 ($E^{\circ\prime}=199.0$ mV) were observed on both the SPCE* and SPCE-P*. The fact that a much smaller ΔE_p of 41 mV for A1/C1 than that of 110 mV for A2/C2 observed indicates that two different electron transfer behaviors of catechol may appear at the SPCE-P*. We thus carried out an experiment to study the dependence of peak current (i_p) on scan rate for these two redox peaks. As shown in Figure 4B, a systematic increase in the peak current (i_p) upon the increase in scan rate was observed at the SPCE-P*. Double logarithmic plots of i_{pa} vs. v for the respective anodic peaks show different slope values of 0.99 and 0.46 for A1 and A2, respectively (Figure 4C). Note that, to understand the exact nature of the oxidation mechanism, a linear plot of (i_{pa} vs. $v^{1/2}$) or (i_{pa} vs. v) represents for the process of diffusion or adsorption controlled reaction, respectively [20]. The value of close to 1 and 0.5 indicates specific adsorption-controlled and diffusion-controlled electron transfer mechanism for the respective redox process. The adsorption characteristics of A1/C1 was further verified by transferring both the SPCE* and SPCE-P* after the reaction in catechol to a blank pH 7 PBS. As can be seen in Figure 4D, sharper and more symmetry redox peaks at the SPCE-P*-CA_{ads} verifies the adsorption of the A1/C1 redox couple. Note that no such a catechol adsorption behavior was observed at a bare SPCE. The ~1.9 fold enhancement of peak current at the SPCE-P*-CA_{ads} to that at the SPCE*-CA_{ads} also verifies the advantage of the simple polishing process to tune up SPCE.

Previously, similar behavior was reported earlier at a catechol-immobilized GCE and the two major symmetric peaks observed were assigned to catechol adsorbed on the surface and the micropore surface, respectively [3]. In our case, the A1/C1 redox peak may stand for the catechol adsorption at the surface and the A2/C2 redox peak for physically entrapped catechol within the pores of the carbon surface at the SPCE-P*-CA_{ads}. With a much simple electrode activation procedure, we can achieve catechol adsorption behavior similar to the earlier observation. Of course, the surface characteristics of the SPCE-P* is essential to achieve such an effective catechol immobilization. It is the presence of γ-Al_2O_3 on carbon surfaces together with the formation of activated carbon surface at the SPCE* largely improve the adsorption of catechol.

3.3 Electrocatalytic Activities

It is well known that the electrochemical oxidation of hydrazine and NADH requires large overpotential at a bare carbon electrode [13,14]. This is indeed the case as hydrazine oxidation occurs at a high potential of 0.80 V at a bare SPCE; whereas, a very small oxidation peak current was observed at ~0.27 V for the SPCE*-CA_{ads}. The overpotential was found to further decrease at the SPCE-P*-CA_{ads} with a dramatic enhancement (~4.05 times) of the anodic peak current compared to that at the SPCE*-CA_{ads} (Figure 5A). A similar electrocatalytic behavior was also observed for the oxidation of NADH with a peak potential of ~0.58 V at a bare SPCE and ~0.24 V at the SPCE-P*-CA_{ads} (Figure 5B). The poor electrocatalytic activity toward the oxidation of hydrazine and NADH at a bare SPCE has been dramatically improved at the SPCE-P*-CA_{ads}.

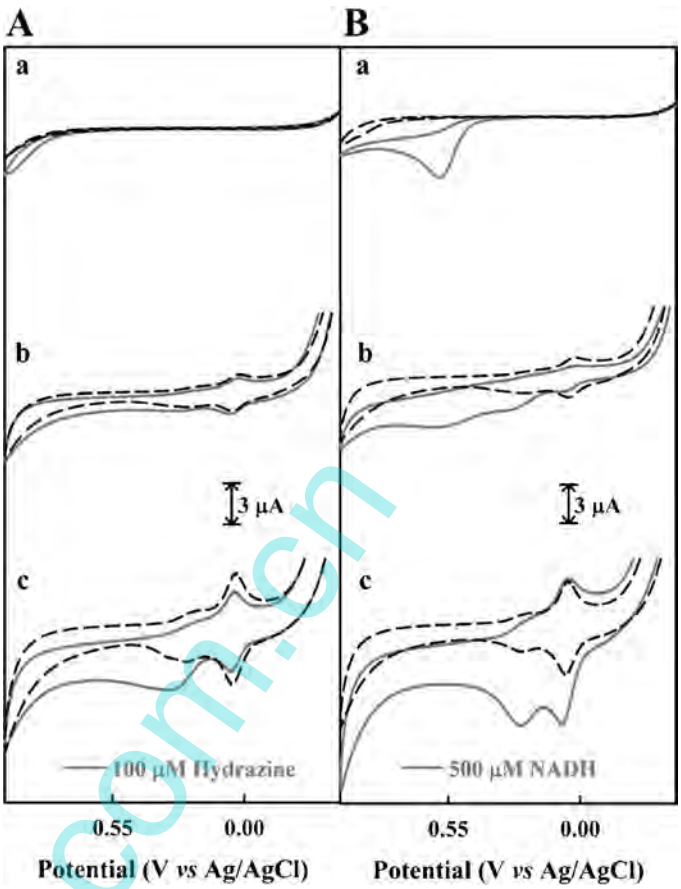

Fig. 5. Cyclic voltammograms in the presence (solid line) and absence (dotted line) of 100 μM hydrazine (A) and 500 μM NADH (B) at a SPCE (a), the SPCE*-CA_{ads} (b) and the SPCE-P*-CA_{ads} (c) in 0.1 M, pH 7 PBS at a scan rate of 10 mV s^{-1}.

To further elucidate the reason for the good electrocatalytic activity toward the oxidation of hydrazine and NADH at the SPCE-P*-CA_{ads}, we measured the surface coverage of catechol (Γ_{CA}). Based on $\Gamma_{CA}=Q_a/nFA$, we observed a much higher value of 0.33 nmol cm^{-2} at the SPCE-P* than that of 0.036 nmol cm^{-2} for the SPCE-P. The fact that there is ~1.9 fold enhancement of the peak current at the SPCE-P*-CA_{ads} compared to the SPCE*-CA_{ads} leads us to believe that both the basal plane sites on which catechol can adsorb and the edge plane sites to facilitate the electrooxidation are equally important [15]. To clarify the activated carbon surface, high resolution XPS was subsequently performed to characterize different surfaces of SPCE, SPCE-P, and SPCE-P*. As shown

www.sjpm.com.cn

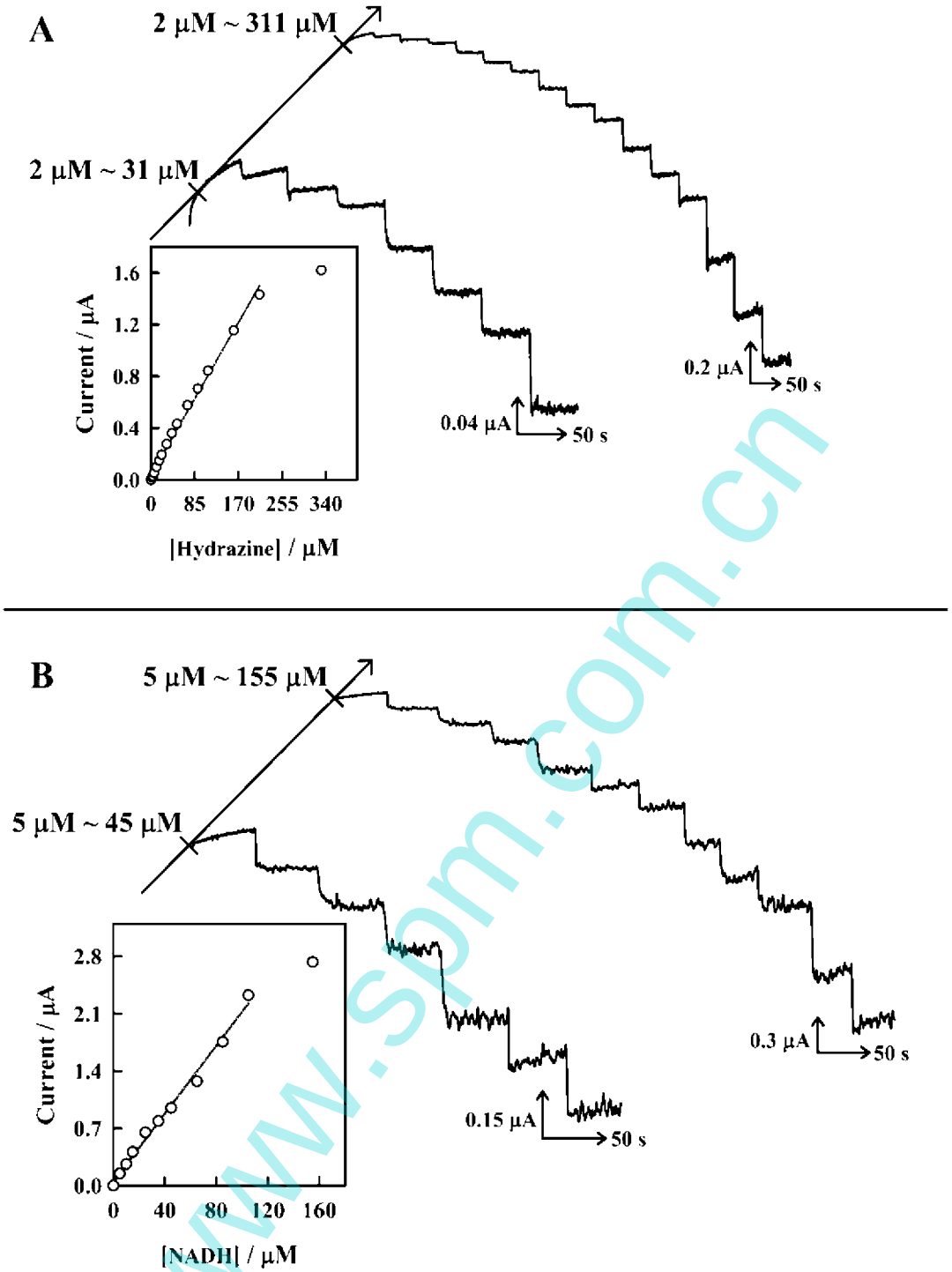

Fig. 6. The amperometric *i–t* curves and calibration plots of hydrazine (A) and NADH (B) at the SPCE-P*-CA_{ads}.

in Table 1, an enrichment of oxygen-containing functional groups at the SPCE-P* was confirmed from the relative proportion of the C–C bond (283.6 eV) versus carbon-oxygen functional groups (C=O for 287.6 eV and C–OH for 285.2 eV) in the XPS spectra [8]. Meanwhile, a covalent linkage mechanism was reported for catechol immobilization in terms of coupling of the C(=O)O– functional group with the oxidized form of the catechol (i.e., *o*-qui-

Table 1. XPS results for different modified SPCE surfaces.

Electrode	Ratio of functional groups	
	C–OH/C–C polymer	C=O/C–C polymer
SPCE	0.56	0.19
SPCE*	0.64	0.26
SPCE-P	0.50	0.17
SPCE-P*	0.60	0.30

www.spm.com.cn

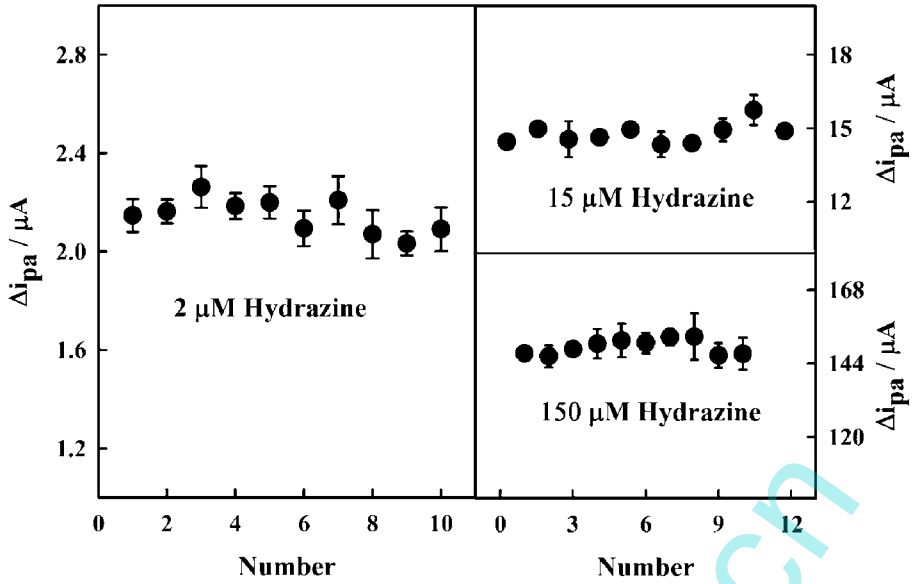

Fig. 7. Reproducibility of the SPCE-P*-CA_{ads} for the detection of 2 μM, 15 μM, and 150 μM hydrazine in 0.1 M pH 7 PBS.

none) [8]. It has also been shown previously that quinoyl groups on GCE together with –COOH groups can increase the electron-transfer rate [16–18]. Our results are in accordance with the proposed concept since the number of –COOH groups present is indeed in the order SPCE-P* > SPCE* > SPCE-P ≈ SPCE.

Figure 6A shows a typical amperometric *i–t* curve of the SPCE-P*-CA_{ads} upon successive addition of hydrazine at an applied potential of 0.30 V. A linear calibration curve over the range from 2 μM to 211 μM hydrazine with a slope of 6.92 μA/mM and a correlation coefficient of 0.993 was obtained. The detection limit was calculated as 0.39 μM ($S/N = 3$). Figure 6B shows the typical amperometric *i–t* curve for NADH with a linear increase from 5 μM to 105 μM. The sensitivity and detection limit were 20.77 μA/mM and 0.81 μM, respectively. The reproducibility of the proposed system was further checked by 5 continuous additions of 2 μM, 15 μM, and 150 μM hydrazine for ten different SPCE-P*-CA_{ads}. As shown in Figure 7, the SPCE-P*-CA_{ads} is stable and reproducible regarding its electrochemical mediation behavior toward the oxidation of hydrazine and NADH. We have successfully demonstrated that the application of the SPCE-P*-CA_{ads} for the detection of NADH and hydrazine and several factors including the increase in hydrophilicity of the carbon architecture cause the difference in sensor performance.

4 Conclusions

We have developed a facile ultrasonic polishing method for the immobilization of catechol on a disposable SPCE. Compared to the conventional approaches of immobilizing catechol on carbon surfaces, our strategy has the following advantages: (i) the mechanical polishing process is capable of improving the micromorphology and surface roughness of the carbon surface; (ii) a highly reproducible SPCE surface can be achieved through this polishing process; (iii) the method is cost-effective and rapid since the carbon activation does not require expensive instruments. The sensitivity and detection limit for NADH of 20.77 μA/mM and 0.81 μM, respectively, are better than those of poly(thionine)-modified carbon electrodes, carbon nanotubes chitosan/GCE, and poly(acrylic acid)-carbon nanotubes complex [21–23]. The sensitivity and detection limit for hydrazine of 6.92 μA/mM and 0.39 μM, respectively, are better than those of coumestan modified carbon paste electrode, DHsalophen/GCE, and PCV chemically modified GCE [24–26].

Acknowledgement

The authors gratefully acknowledge financial support from the *National Science Council of Taiwan*.

References

[1] F. Pariente, E. Lorenzo, H. D. Abruna, *Anal. Chem.* **1994**, *66*, 4337.
[2] A. A. J. Torriero, H. D. Piola, N. A. Martinez, N. V. Panini, J. Raba, J. J. Silber, *Talanta* **2007**, *71*, 1198.
[3] N. A. Martinez, G. A. Messina, F. A. Bertolino, E. Salinas, J. Raba, *Sens. Actuators B* **2008**, *133*, 256.
[4] A. Salimi, R. Hallaj, *Electroanalysis* **2004**, *16*, 1964.
[5] H. R. Zare, N. Nasirizadeh, *Electrochim. Acta* **2007**, *52*, 4153.
[6] C. D. Allred, R. L. McCreery, *Anal. Chem.* **1992**, *64*, 444.
[7] A. Salimi, L. Miranzadeh, R. Hallaj, *Talanta* **2008**, *75*, 147.
[8] A. S. Kumar, S. Sornambikai, P. Gayathri, J.-M. Zen, *J. Electroanal. Chem.* **2010**, *641*, 131.

 © 2013 Wiley-VCH Verlag GmbH & Co. KGaA, Weinheim

www.sjm.com.cn

[9] M. Li, Y.-T. Li, D.-W. Li, Y.-T. Long, *Anal. Chim. Acta* **2012**, *734*, 31.
[10] J. P. Metters, R. O. Kadara, C. E. Banks, *Analyst* **2011**, *136*, 1067.
[11] J. Zak, T. Kuwana, *J. Am. Chem. Soc.* **1982**, *104*, 5514.
[12] S. Dong, T. Kuwana, *J. Electrochem. Soc.* **1984**, *131*, 813.
[13] A. A. Ensafi, E. Mirmomtaz, *J. Electroanal. Chem.* **2005**, *583*, 176.
[14] D.-W. Yang, H.-H. Liu, *Biosens. Bioelectron.* **2009**, *25*, 733.
[15] Q. Li, C. Batchelor-McAuley, R. G. Compton, *J. Phys. Chem. B.* **2010**, *114*, 7423.
[16] S. H. DuVall, R. L. McCreery, *J. Am. Chem. Soc.* **2000**, *122*, 6759.
[17] I. Dumitrescu, N. R. Wilson, J. V. Macpherson, *J. Phys. Chem. C* **2007**, *111*, 12944.
[18] A. F. Holloway, G. G. Wildgoose, R. G. Compton, L. Shao, M. L. H. Green, *J. Solid State Electrochem.* **2008**, *12*, 1337.
[19] G. N. Kamau, W. S. Willis, J. F. Rusling, *Anal. Chem.* **1985**, *57*, 545.
[20] A. J. Bard, L. R. Faulkner, *Electrochemical Methods, Fundamentals, and Applications*, 2nd ed., Wiley, New York **2001**.
[21] H. R. Zare, N. Nasirizadeh, *Electroanalysis* **2006**, *18*, 507.
[22] R.-P. Monica, E. Lorenzo, F. Pariente, *Sens. Actuators B* **2005**, *107*, 678.
[23] S. M. Golabi, H. R. Zare, M. Hamzehloo, *Microchem. J.* **2001**, *69*, 111.
[24] S. Baskar, J.-L. Chang, J.-M. Zen, *Biosens. Bioelectron.* **2012**, *33*, 95.
[25] M. Zhang, A. Smith, W. Gorski, *Anal. Chem.* **2004**, *76*, 5045.
[26] A. Liu, T. Watanabe, I. Honma, J. Wang, H. Zhou, *Biosens. Bioelectron.* **2006**, *22*, 694.

www.spm.com.cn